Petroleum Science 23 (2026) 5984–5991

Contents lists available at ScienceDirect

Petroleum Science

journal homepage: www.keaipublishing.com/en/journals/petroleum-science

Original Paper

Potential origin of natural vanadium hydride in the Earth's shallow mantle

Yu-Tong Su [a,b], Zhi-Jun Jin [a,c,*], Ren-Biao Tao [b,c], Jin-Tao Zhu [b], Run-Chao Liu [a,c], Lu Wang [a], Hao-Zhe Zhang [a], Shubham Choudhary [b]

[a] Institute of Energy, Peking University, Beijing, 100871, China
[b] Center for High Pressure Science and Technology Advanced Research, Beijing, 100193, China
[c] Peking University Ordos Institute of Energy, Ordos, 017010, Inner Mongolia, China

ARTICLE INFO

Article history:
Received 8 August 2025
Received in revised form
25 December 2025
Accepted 6 April 2026
Available online 8 April 2026

Edited by Min Li

Keywords:
Natural metal hydrides
High-temperature and high-pressure experiments
Vanadium hydride
Crust-mantle interaction
Deep water cycle

ABSTRACT

Metal hydrides have emerged as promising candidates for energy storage in clean hydrogen systems. While these materials are typically synthesized under controlled laboratory conditions, naturally occurring vanadium hydride (VH_2) has been identified in mantle-derived igneous rocks, suggesting that it may from in geological environments. In this study, we investigate the formation mechanisms and melting behavior of vanadium hydride under mantle conditions by integrating high-pressure experimental techniques with molecular dynamics simulations. Our experimental results demonstrate that hydrous minerals, such as $Mg(OH)_2$, can react with elemental vanadium (V_0) at elevated temperatures (1000–1500 °C) and pressures (0.8–3 GPa) to form vanadium hydride. Molecular dynamics simulations further reveal that the melting temperature of VH_2 at 1 GPa ranges between 1400 and 1500 °C. These findings suggest that natural vanadium hydride may originate in the Earth's shallow mantle and subsequently migrate to the crust or surface through magmatic processes. This study provides a theoretical basis for further exploration of naturally occurring metal hydrides and supports the development of synthetic metal hydrides for solid-state hydrogen storage.

1. Introduction

Nowadays, the global economy's reliance on fossil fuels is a critical challenge. Not only are fossil fuel resources rapidly being depleted (Luo et al., 2015), but the harmful effects of these fuels, such as greenhouse gas emissions and resulting environmental problems, are increasingly recognized (Yue et al., 2021). Consequently, it is essential to reassess the current reliance on fossil fuels and to make appropriate policy changes to support sustainable energy, including reducing carbon dioxide emissions, ensuring energy security, and fostering the development of new industrial and technological energy bases (Karlsruhe, 2003; Durbin and Malardier-Jugroot, 2013).

Compared with traditional energy storage techniques, solid-state hydrogen storage offers higher energy efficiency, greater safety, and superior volumetric and gravimetric storage capacities. Additionally, solid storage materials offer the potential advantages of absorption and desorption capabilities at moderate temperatures (approximately 300 °C) and pressures between 1 and 10 bar (AbdKhalim Khafidz et al., 2016). As efficient solid hydrogen storage materials, metal hydrides have been extensively studied in the field of materials science (Sakintuna et al., 2007). Metal hydrides typically form at relatively low temperatures and high pressures, and hydrogen release from them is an endothermic process (Jain et al., 2007). Therefore, hydrogen can be released from metal hydrides by increasing the temperature or lowering the external pressure (Jain et al., 2010).

Notably, metal hydrides can naturally occur in Earth's and planetary interiors, which has attracted significant attention in previous studies. For example, previous high-temperature and high-pressure experimental studies have demonstrated that hydrogen exhibits a strong affinity for iron, readily forming iron-

* Corresponding author.
E-mail address: jinzj1957@pku.edu.cn (Z.-J. Jin).
Peer review under the responsibility of China University of Petroleum (Beijing).

https://doi.org/10.1016/j.petsci.2026.04.006

hydrogen compounds in Earth's deep mantle and even in the core (Mao and Hu, 2017). Yuan et al. also found that hydrogen exhibits strong iron affinity under high pressure (Yuan and Steinle-Neumann, 2020). Consequently, the core is considered to have the largest hydrogen reservoir on Earth (Wang et al., 2021). Umemoto et al. found that a hydrogen concentration of about 1 wt% may exist in the Earth's outer core (Umemoto and Hirose, 2015), Thompson et al. found that the Earth's outer core may contain up to 0.8–1.3 wt% hydrogen based on the density and velocity of iron hydrides with different stoichiometries matching the PREM (Preliminary Reference Earth Model) (Thompson et al., 2018). High-pressure experimental studies also suggest a significant positive correlation between hydrogen solubility in iron and pressure, indicating that as pressure decreases, iron-hydrogen compounds in the deep mantle and core will gradually decompose, releasing hydrogen molecules (Tagawa et al., 2021). Recent studies have also indicated that hydrogen may be an essential component of the metallic cores of terrestrial planets and their satellites with masses greater than 10% of Earth (Tagawa et al., 2021). Even beyond our solar system, chromium hydride (CrH) has been detected in the hot Jupiter WASP-31b (Braam et al., 2021), and iron hydride (FeH) has been observed in the gas giant exoplanet KELT-9b (Changeat and Edwards, 2021).

Besides iron hydrides, Suzuki et al. (1989) systematically studied the formation of transition metals (e.g., Fe, Co, Ni, Mn, V, Ti, Cr) hydrides under pressure (*P*) -Temperature (*T*) conditions of 5 GPa and 1000–1300 °C. Their experimental results showed that metal hydrides can be formed by reacting water with metals or metal oxides at high pressure and temperature. However, upon quenching and recovery, the hydrides of iron, cobalt, and nickel decomposed, releasing hydrogen, indicating instability at atmospheric pressure. In contrast, the hydrides of titanium, vanadium, chromium, and manganese can be quenched and recovered at atmospheric pressure and remain stable (Suzuki et al., 1989). Despite growing interest in the study of natural metal hydrides, the understanding of their properties in the Earth's interior is still limited compared to other natural energy substances, such as coal and petroleum.

This study examines the formation mechanisms and stability of vanadium hydride under high-pressure, high-temperature conditions similar to those found in Earth's shallow mantle. Experimental simulations were conducted using a piston-cylinder apparatus to examine vanadium-hydrogen compound formation in three distinct chemical systems: V_0-$CaSiO_3$-$SiO_2{\cdot}xH_2O$-$Ca(OH)_2$, V_0-Mg_2SiO_4-SiO_2-$Mg(OH)_2$, and V_0-MgO-SiO_2-$Mg(OH)_2$. Our novel findings investigate the pressure-temperature of vanadium hydride compound formation in Earth's shallow mantle. Molecular dynamics simulations were performed to determine the melting behavior of VH_2 at 1 GPa, providing crucial insights into its thermal stability in mantle environments. These findings have significant implications for understanding the potential migration of vanadium hydrides via mantle-derived magmatic processes.

2. Materials and studying methods

2.1. Starting materials

This study employed experiments on the $CaSiO_3$-$SiO_2{\cdot}xH_2O$-$Ca(OH)_2$-V_0 (CSHV) system, using the same initial composition as in a previous study (Suzuki et al., 1989), in which the experimental P was reduced to explore the pressure conditions of V-H compounds. Given that Earth's interior primarily consists of a magnesium-silicate environment rich in olivine, we also used the MgO-SiO_2-Mg $(OH)_2$-V_0 (MSHV) system in our simulations. The starting materials included vanadium metal powder (purity >99.5%), SiO_2 (purity >99%), $SiO_2{\cdot}xH_2O$ (purity >99%), $Ca(OH)_2$ (purity >99%), Mg_2SiO_4 powder (purity >99.5%), $Mg(OH)_2$ (purity >99%), and MgO (purity >99%). All starting materials were mixed in a mortar with anhydrous ethanol at the specified ratio for 60 min, then placed in a 50 °C oven for 10 min to ensure sample uniformity. The reaction details are shown in Table 1.

2.2. High-pressure experimental synthesis and characterization

All high-pressure experiments were conducted using a TK-PC-I piston-cylinder apparatus at HPSTAR (Center for High Pressure Science & Technology Advanced Research). The homogeneous powder was packed into precious-metal tubes with an inner diameter of 2.2 mm and a length of 7 mm, and the ends were sealed using a spot-welding machine. Except for Run-3, which used a gold capsule as the reaction vessel, platinum capsules were used for all other reactions. The sealed capsules were placed in a magnesium oxide sleeve, with an outside graphite tube serving as the heating element. The operating temperature was measured using a Type C thermocouple and controlled to within 1 °C. The runs were quenched at ~250 °C/s by cutting off the power. Detailed experimental assembly is shown in Fig. S1.

After each experiment, the capsules were longitudinally cut open and mounted in epoxy resin for further characterization. The microstructure was examined using a scanning electron microscope (SEM) at 15 kV acceleration voltage and 10 nA beam current in a JEOL JSM-7500F, and at 20 kV acceleration voltage in a ZEISS Gemini 300.

Due to the analytical limitations of SEM-EDS for hydrogen and helium, EDS cannot be used to analyze these elements. The nuclei of these elements each have only one neutron, so there are no free electrons to emit. We used Tof-SIMS to characterize the vanadium granules. Characterization of H for our experimental products was

Table 1
Summary of experimental conditions.

Systems	Number	Starting materials	Temperature, °C	Pressure, GPa	Time
CSHV	Run-1	8V + $CaSiO_3$+2$SiO_2{\cdot}xH_2O$ +2$Ca(OH)_2$	1300	3	10 min
	Run-2	8V + $CaSiO_3$+2$SiO_2{\cdot}xH_2O$ +2$Ca(OH)_2$	1300	3	1 h
	Run-3	8V + $CaSiO_3$+2$SiO_2{\cdot}xH_2O$ +2$Ca(OH)_2$	1000	3	1 h
MSHV	Run-4	Mg_2SiO_4+3SiO_2+2 $Mg(OH)_2$+6V	1200	1	1 h
	Run-5	Mg_2SiO_4+3SiO_2+2 $Mg(OH)_2$+6V	1200	3	1 h
	Run-6	8MgO+6SiO_2+2 $Mg(OH)_2$+4V	1000	1	2.5 h
	Run-7	8MgO+6SiO_2+2 $Mg(OH)_2$+4V	1000	1	48 h
	Run-8	8MgO+6SiO_2+2 $Mg(OH)_2$+4V	1200	1	1.5 h
	Run-9	8MgO+6SiO_2+2 $Mg(OH)_2$+4V	1200	0.8	4.5 h
	Run-10	8MgO+6SiO_2+2 $Mg(OH)_2$+4V	1250	1	16 h
	Run-11	8MgO+6SiO_2+2 $Mg(OH)_2$+4V	1200	1	28 h
	Run-12	8MgO+6SiO_2+2 $Mg(OH)_2$+4V	1200	1	48 h

performed using a TOF-SIMS 5-100 instrument from IONTOF GmbH at Tsinghua University. The epoxy-resin-mounted targets were affixed to the sample stage using a conductive adhesive and then pre-evacuated in a vacuum chamber. Once the pressure in the pre-vacuum chamber reached below 2×10^{-5} Pa, the samples were transferred to the main vacuum chamber, which maintained a pressure of 3.6×10^{-6} Pa throughout the experiment. Surface contamination was removed by sputtering the sample surface with a sputter gun under ultra-high vacuum, and data were collected in high-spatial-resolution (fast) mode. Fast-mode parameters included a primary ion beam with Bilt at 30 keV. The scan area ranged from 30 μm × 30 μm to 100 μm × 100 μm. Depth-profiling parameters included an Arnt cluster ion sputter gun operated at 10 keV, with depth profiling conducted for 900 s at sputtering rates of 0.17 or 0.451 nm/s (SiO_2 equivalent). The use of Arnt cluster ions avoided changes such as surface oxidation caused by the sputtering beam.

2.3. Molecular dynamics simulation

The calculations of density functional theory (DFT) are done with the projector augmented plane-wave basis, which is implemented in Vienna ab-initio simulation package (VASP) (Kresse and Joubert, 1999). The plane waves are cut off at 250 eV. The exchange-correlation of electrons is described using the generalized gradient approximation (GGA), as proposed by Perdew, Burke, and Ernzerhof (Perdew et al., 1996). The DFT-D3 approach is used to capture long-range van der Waals interactions (Grimme et al., 2010). The energy convergence criterion for solving self-consistent Kohn-Sham equations is 10^{-5} eV. The Brillouin zone is sampled with resolutions better than 0.03 $Å^{-1}$, using the scheme of Monkhorst-Pack (Monkhorst and Pack, 1976). To study the melting of VH_2, molecular dynamics simulations are conducted in the NpT ensemble using a Langevin thermostat, as implemented in VASP. The systems are allowed to exhibit thermal fluctuations in pressure and temperature around their equilibrium values. The time interval utilized in the molecular dynamics simulation is 0.5 fs. A 20 ps thermalization is performed at each temperature to drive the system into thermal equilibrium. A series of 5 ps simulations is performed to sample data. The melting point is predicted by observing the abnormal point in the temperature evolutions of the diffusion factor and potential energy (Sun et al., 2020). The CIF file of the VH_2 crystal comes from Bindi et al. (2020).

Solid melting has an overheating effect, which generally leads to an overestimation of the melting point. However, in our simulation, overheating due to insufficient kinetic energy is not possible because the kinetic energy in our model is not fixed; the system's kinetic energy exchanges with the hot melt, which exhibits considerable fluctuations. When the system reaches the melting point, it can melt and absorb the kinetic energy of the hot melt.

3. Results and discussions

3.1. Formation of VH_x in CSHV and MSHV systems at Earth's mantle conditions

In the CSHV system, synthetic samples consist of two components: dark silicate minerals and light-coloured granules, which are mainly composed of vanadium (V) as determined by SEM-EDS. Within individual V granules, we observed compositional heterogeneity: some areas appeared bright, whereas others appeared dark, indicating the presence of two distinct products. Fig. 1 shows the distribution of hydrogen and oxygen on Tof-SIMS images in the CSHV system.

ptHydrogen and oxygen were detected throughout the vanadium granule, indicating successful synthesis of vanadium-

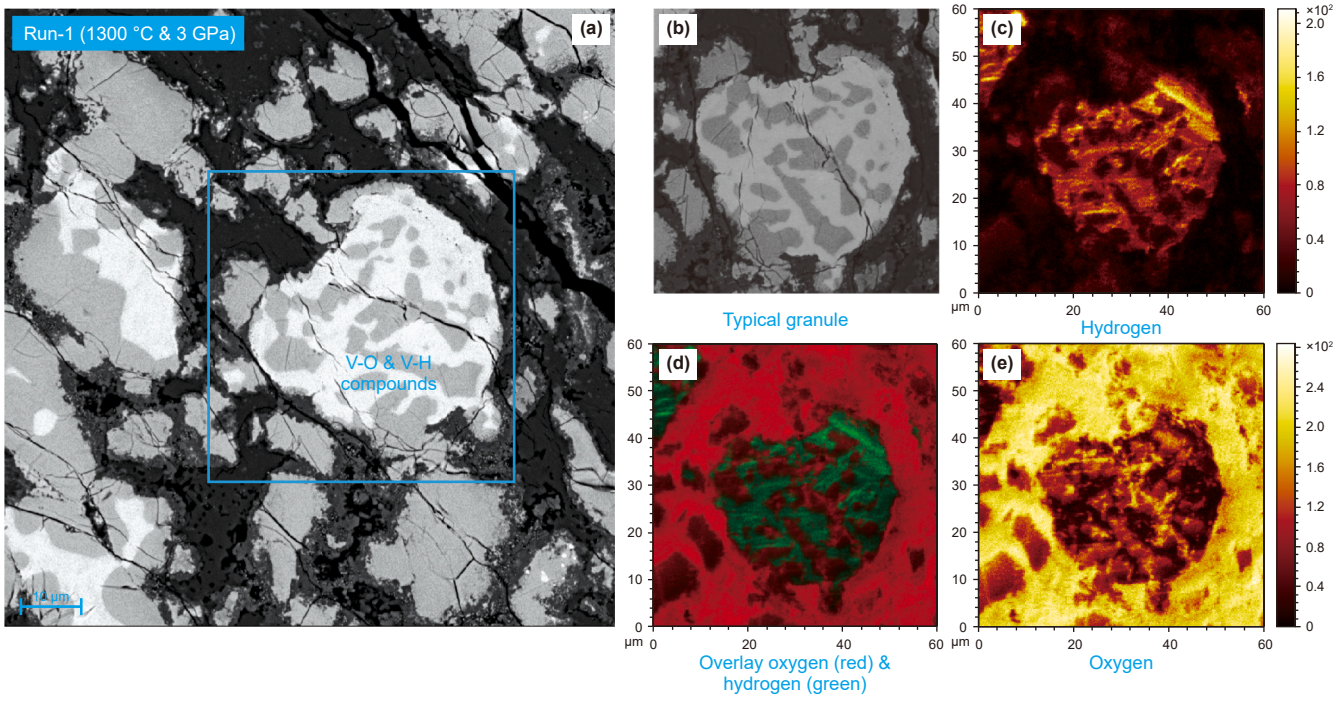

Fig. 1. A typical SEM-EDS and Tof-SIMS map on the V-rich granule in the CSHV system (1300 °C-3 GPa-10 min). **(a)** Scanning electron microscope image of a typical granule and the surrounding matrix; **(b)** Scanning electron microscope image of a typical granule; **(c)** Tof-SIMS surface scan distribution map of oxygen in vanadium granules; **(d)** Overlay of hydrogen and oxygen in vanadium granules, where red is the distribution area of oxygen and green is the distribution area of hydrogen; **(e)** Tof-SIMS surface scan distribution map of hydrogen in vanadium granules.

hydrogen compounds. We observed coexistence of hydrogen and oxygen within vanadium granules in the Tof-SIMS map, confirming the presence of both vanadium-hydrogen and vanadium-oxide compounds. Our experimental results demonstrate that vanadium-hydrogen compounds can be synthesized and remain stable after quenching, consistent with previous studies (Suzuki et al., 1989). Suzuki et al. used $8V_0 + CaSiO_3 + 2SiO_2{\cdot}xH_2O + 2Ca(OH)_2$ as the initial components and reacted them at 5.3–5.4 GPa and above 1300 °C for 10 min or 1 h. Their experiments produced $(VH_{1.9} + VO_x) + (Ca, Mg)SiO_3 + Gar$ (+unk), indicating that hydrogen and oxygen coexist in vanadium at high temperature and pressure.

Compared with Suzuki et al.'s initial conditions at 5 GPa, our experiments in the CSHV system were conducted at 3 GPa. Fig. 2 presents details of our research, compared with previous studies.

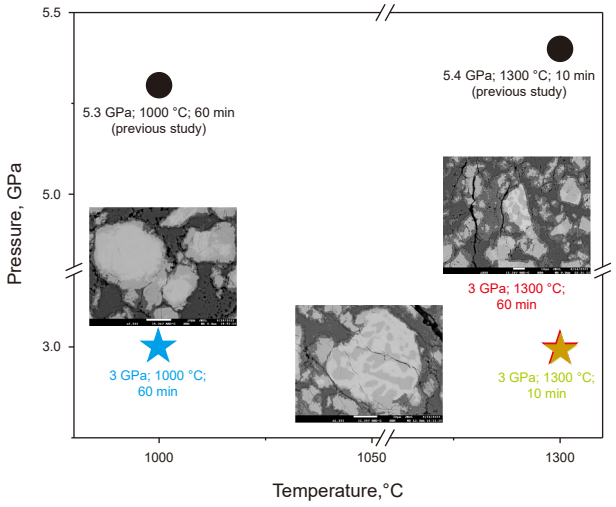

Fig. 2. Comparison of the CSHV system with previous studies (Suzuki et al., 1989).

This establishes a new lower pressure limit for vanadium-hydrogen compounds. Additionally, the differences in reaction duration (10 min versus 1 h) and temperature (1000 °C versus 1300 °C) appear to have a relatively small impact on hydrogen incorporation into vanadium, as no significant differences in hydrogen content were observed in Figs. 1 and S2. This suggests that most of the reaction occurred within the first 10 min.

Fig. 3 shows that the experimental products of the MSHV system also exhibit the light and dark areas within a single vanadium granule, as in the CSHV system. The light-coloured areas in the SEM-BSE image correspond to vanadium hydrogen compounds, while the dark-coloured areas correspond to vanadium oxide compounds. This is consistent with CSHV system results, indicating that metal hydrides can also be produced in the MSHV system under such temperature and pressure conditions.

In the MSHV system, under experimental conditions at 0.8 GPa, we also observed coexistence of vanadium-hydrogen and vanadium-oxide phases within vanadium granules. Previous studies have shown that at 5 GPa and 1000–1300 °C in the CSHV system (Suzuki et al., 1989), vanadium could react with water under high temperatures and high pressures to form metal hydrides. In our experiments, we further decreased the pressure to 0.8 GPa in the MSHV system. Still, we observed the formation of vanadium-hydrogen compounds (introducing water through hydrated silica in the CSHV system and through magnesium hydroxide in the MSHV system). This indicates that the required pressure for vanadium metal to react with water to form vanadium hydrides may be lower than previously thought. However, the specific temperature and pressure boundary for V-H formation has not yet been determined. This still requires further exploration.

3.2. *Melting of VH_2 at high-pressure conditions relevant to Earth's shallow mantle*

This study explored the melting behavior of VH_2 at 1 GPa to delineate its melting curve by molecular dynamics simulations.

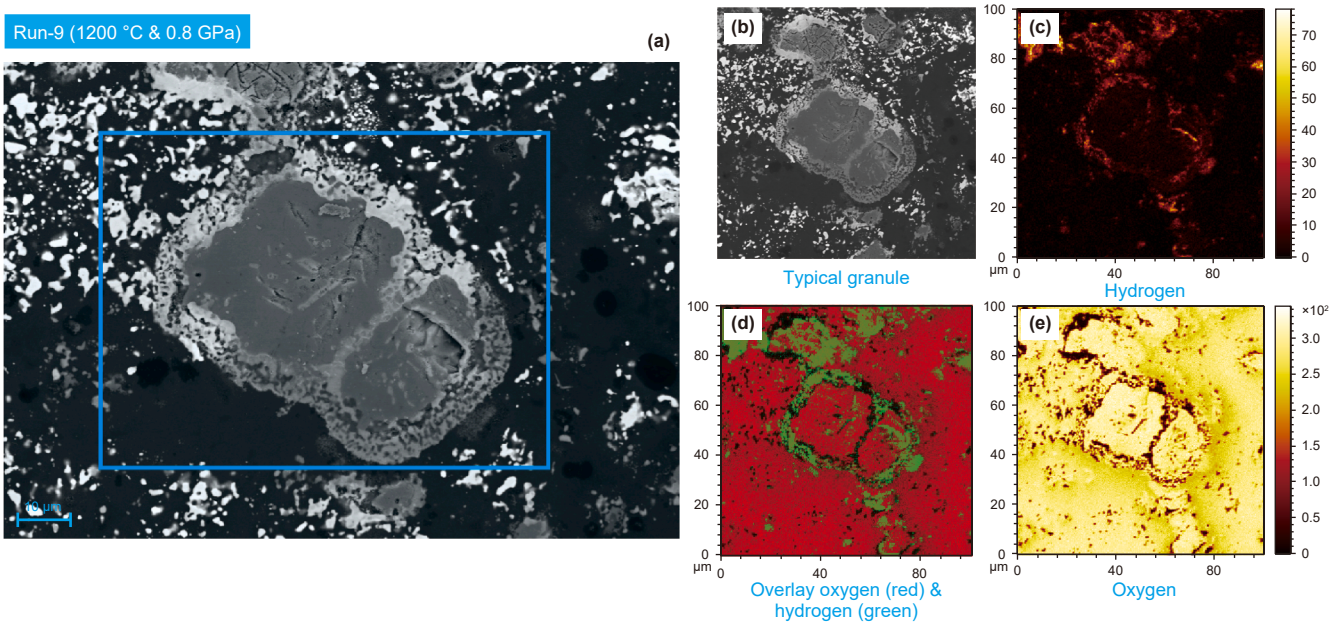

Fig. 3. A typical SEM-EDS and Tof-SIMS map on the V-rich granule in the MSHV system (1200 °C-0.8 GPa-4.5 h). **(a)** Scanning electron microscope image of a typical granule and the surrounding matrix; **(b)** Scanning electron microscope image of a typical granule; **(c)** Tof-SIMS surface scan distribution map of oxygen in vanadium granule; **(d)** Overlay of hydrogen and oxygen in vanadium granules, where red is the distribution area of oxygen and green is the distribution area of hydrogen; **(e)** Tof-SIMS surface scan distribution map of hydrogen in vanadium granules.

The melting behavior of VH_2 was simulated at heating rates of 0.004 K/fs at 800, 1000, 1200, and 1400 °C, and 0.002 K/fs at 1500 and 1600 °C. The green section represents the potential energy-temperature curve shown in Fig. 4. At a pressure of 1 GPa, the potential energy remains relatively stable over the temperature range 800–1400 °C. However, the increase between 1400 and 1500 °C indicates a step change attributable to the latent heat of phase transition in the VH_2 system. Beyond 1500 to 1600 °C, the slope of the potential energy change decreases, advocating the melting point of VH_2 to fall between 1400 and 1500 °C based on potential energy changes. In the blue section of Fig. 4, the diffusion coefficient of the VH_2 system at 1 GPa shows a marked increase from less than 2 (1.987 $\mu m^2/s/atom$) to greater than 2.5 (2.563 $\mu m^2/s/atom$) over the 1400–1500 °C range.

In addition, we simulated the cutoff energy of 500 eV. We also simulated the radial distribution function and the atomic pair distribution function. As shown in Fig. S6(a), for temperatures below 1400 °C, radial distribution function exhibits characteristic peaks near ~1.8 Å, ~3.5 Å, and ~4.7 Å, indicating that the system has long-range structural order unique to crystals; for temperatures above 1500 °C, radial distribution function only exhibits characteristic peaks near ~1.8 Å and ~3.2 Å, indicating that the system is in a liquid phase with only short-range structural order. Therefore, the melting point of the system is between 1400 and 1500 °C. As shown in Fig. 6(b), (c), (d), for temperatures below 1400 °C, V-V, H-H, V-H and other atomic pairs can all show characteristic peaks near 5 Å, indicating that the system has a long-range structural order unique to crystals; for temperatures above 1500 °C, the distinctive peaks of various atomic pairs near 5 Å day sharply. In particular, for V-H atomic pairs (the main bonding type of VH_2 compounds), the characteristic peaks at ~3.5 Å and ~4.7 Å disappear entirely, indicating that the system has entered a long-range disordered liquid phase. Therefore, the melting point of the system is between 1400 and 1500 °C.

Fukai (2005) conducted experiments to constrain the high-pressure melting curve of vanadium metal up to 5 GPa. Zhao et al. (2019) further simulated various phase diagrams for vanadium-hydrogen, indicating the stability region of VH_2.

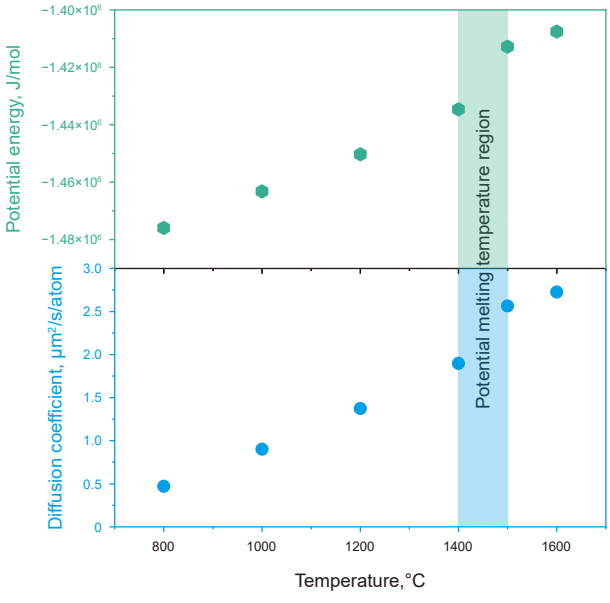

Fig. 4. The melting point of obtained by molecular dynamics simulation. The green area represents the VH_2 potential energy calculated at 1 GPa; the blue area represents the VH_2 diffusion coefficient calculated at 1 GPa.

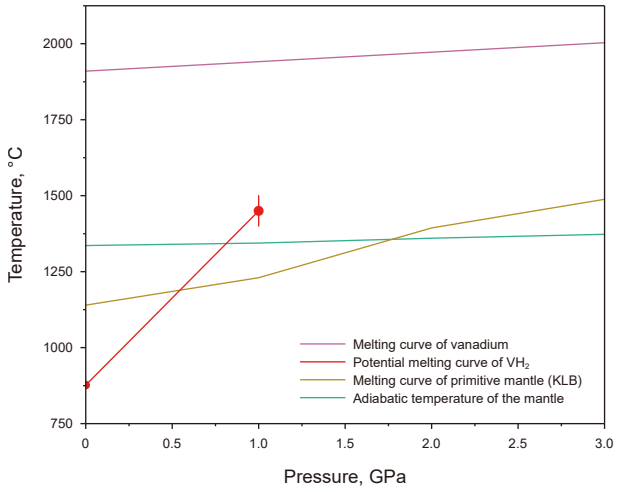

Fig. 5. Comparison of the melting curve of VH_2 with that of vanadium, the mantle melting curve, and the adiabatic curve of the mantle. The purple line represents the high-pressure melting curve of vanadium calculated by Zhang et al. (2020), and the red line represents the possible melting range of VH_2 at 1 GPa in this study. The leftmost red dot represents the melting point of VH_2 at atmospheric pressure calculated by Hong et al. (2022), while the rightmost red dot, taken from the midpoint of the range calculated in this study, is for comparison purposes. The brown line represents the primitive mantle melting curve (Takahashi, 1986); the green line represents the adiabatic temperature of the mantle (Katsura, 2022).

However, there are few studies on the phase diagram of vanadium at pressures below 5 GPa. The melting point of metallic vanadium continuously rises from an initial 1910 °C (Zhang et al., 2020). Compared to pure vanadium metals, vanadium hydrides show significantly lower melting temperatures at similar pressures (i.e., 1 GPa). Fig. 5 shows the distribution of these curves. Bindi et al. (2019) estimated the formation conditions of VH_2 at around 1 GPa and 1450–1500 °C, with the minimum temperature being above 1150 °C. Subsequently, V-H-rich silicate melt migrates and ascends to the surface in a hydrogen-methane (H_2-CH_4) atmosphere.

This estimation is in agreement with the melting point of VH_2 as validated through our computational simulations.

3.3. *Possible formation model of vanadium hydride compounds in the shallow mantle*

The geochemical evolution of vanadium on Earth originated from planetary accretion processes and subsequent core-mantle differentiation. Cosmochemical estimates indicate a Bulk Earth vanadium concentration of 95 mg/kg, with the metallic core containing approximately 120 mg/kg (McDonough and Sun, 1995). Experimental petrology studies demonstrate that vanadium exhibited strong siderophile behavior during early magma ocean crystallization, preferentially partitioning into the metallic core under reducing conditions and high pressures (Geβmann and Rubie, 1998). Recent geochemical models suggest the core may sequester up to 50% of Earth's total vanadium inventory (McDonough, 2003). As a redox-sensitive transition metal, vanadium displays multiple valence states (+2 to +5) in geological systems (Shearer et al., 2006). Notably, native vanadium (V_0) has been identified in high-temperature volcanic sublimates from Colima volcano, Mexico (Ostroumov and Taran, 2016), and as inclusions within mantle-derived minerals (Griffin et al., 2020). These findings suggest that it is not entirely impossible to find elemental vanadium in Earth's mantle, indicating that there are

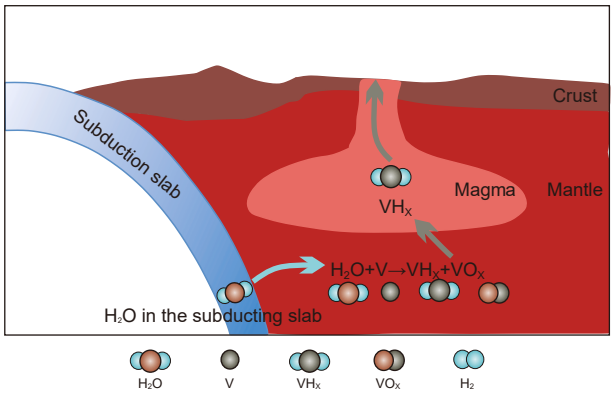

Fig. 6. Potential formation mechanism of vanadium hydride in the shallow mantle. Water reacts with metallic vanadium in the mantle to form vanadium hydrides and vanadium oxides, and the vanadium hydrides are subsequently transported toward the Earth's surface with ascending magmas.

geological conditions within the Earth that could potentially be suitable for the existence of metallic vanadium.

Geochemical estimates by Ohtani (2019) indicate significant water storage capacity within Earth's mantle, with approximate reservoirs of 0.04, 0.2–1, and less than 2 ocean masses in the upper mantle, transition zone, and lower mantle, respectively. The coexistence of metallic vanadium with these substantial water reservoirs under appropriate thermobaric conditions establishes a geochemically plausible environment for the formation of vanadium-hydrogen compounds.

Subduction zones serve as primary conduits for deep-Earth water recycling, playing a pivotal role in global water cycles. Water is initially transported into subduction systems primarily through mineral-bound forms within hydrous phases of the oceanic lithosphere. Progressive metamorphic dehydration reactions release water along the subduction path as pressure-temperature (*P-T*) conditions evolve. Experimental petrology demonstrates that water liberation occurs across an extensive depth range (~30–150 km, corresponding to 1–5 GPa) (Wang et al., 2019). Notably, a considerable fraction remains chemically bound within subducted sediments, crustal materials, and potentially the uppermost mantle of the descending slab (van Keken et al., 2011).

Experimental studies demonstrate that metallic vanadium exhibits significant hydrogen solubility, reaching up to 800 ppm under ambient conditions (Smith and Peterson, 1982). This solubility exhibits positive correlations with both pressure and temperature (Kumar et al., 2012). In our experimental simulations of the CSHV and MSHV systems, water was introduced through hydrous silica ($SiO_2{\cdot}xH_2O$) and magnesium hydroxide ($Mg(OH)_2$) precursors. Under the experimental *P-T* conditions, thermal decomposition of $Mg(OH)_2$ yielded MgO and H_2O (Fig. S3).

Microanalytical evidence from Figs. 1 and 3 reveals the coexistence of hydrogen and oxygen within individual vanadium grains, suggesting the following redox reaction under high *P-T* conditions: $V + H_2O \rightarrow VH_x + VO_x$. These findings support two potential formation pathways for mantle vanadium hydrides: reaction between metallic vanadium and primordial water in early terrestrial magmas, or interaction between vanadium and fluids derived from dehydration of subducted hydrous minerals. Fig. 6 presents a conceptual model illustrating these formation mechanisms.

Based on current understanding, we propose a potential formation mechanism whereby metallic species (e.g., elemental vanadium) present in Earth's mantle may undergo redox reactions with slab-derived fluids under specific thermobaric conditions to form stable metal hydrides. While hydrides of siderophile elements (e.g., Fe, Co, Ni) are thermodynamically unstable upon decompression during mantle convection and may dissociate into their metallic and hydrogen components, certain metal hydrides demonstrate sufficient stability to survive magmatic transport from mantle depths to the surface environment.

3.4. The significance of natural metal hydride in clean energy

Metal hydrides are gaining increasing attention as an excellent means of solid-state hydrogen storage. The low-cost methods for producing metal hydrides are a key area of ongoing research. Storing hydrogen in solid form is a safe approach to reducing storage pressure, thereby enhancing safety. Solid-state hydrogen storage can be classified into two categories: physical adsorption and chemical adsorption. In physical adsorption, hydrogen molecules are adsorbed onto the surfaces of highly porous materials, such as metal-organic frameworks (MOFs) and carbon-based materials. In chemical adsorption, hydrogen reacts with the storage material to form composite hydrides, chemical hydrides, and/or metal hydrides (Tseng et al., 2023).

Vanadium and vanadium-based alloys have been widely studied as candidate materials for hydrogen storage and permeation applications. Compared with other metals that form hydrides, such as titanium, uranium, and zirconium, metallic vanadium exhibits superior hydrogen-storage properties. Vanadium exhibits high hydrogen solubility and diffusion rates under nominal temperature and pressure conditions. Currently, solid-state applications of vanadium primarily involve synthesizing vanadium alloys with other metals for hydrogen storage. The addition of other elements not only reduces costs but also alters hydrogenation performance, including dissociation pressure and hydrogen storage capacity (Kumar et al., 2017).

The world's first natural hydride, VH_2, has demonstrated a hydrogen storage efficiency of 3.5 wt%, which exceeds that of some artificially synthesized products. The hydrogen storage efficiency of various compounds is as follows: Mg_3Ag (2.1 wt%) (Si et al., 2013); Mg_2Cu (2.6 wt%) (Aguey-Zinsou and Ares-Fernández, 2010); Mg_3Cd (2.8 wt%) (Skripnyuk and Rabkin, 2012); $TiCr_2H_4$ (2.57 wt%) (Chen et al., 2005); $V_{22}Ti_{35}Cr_{43}$ (2.5 wt%) (Mazzolai et al., 2008). The unique chemical properties of vanadium make it highly suitable for various industrial and scientific applications. As the world shifts towards a hydrogen fuel-based economy, there are challenges due to the lack of technology for large-scale production of metal hydrides (Kumar et al., 2022). Although the gravimetric hydrogen storage density of VH_2 is not very promising, its volumetric hydrogen storage density is relatively superior compared to the listed hydrogen storage materials (Fig. S4).

Suzuki's experiments showed that the hydrides of Fe, Co, and Ni are not stable after quenching (Suzuki et al., 1989). Furthermore, the computational studies by Smithson et al. (2002) have calculated the formation energies of common transition metals, revealing that in addition to V, Ti, Cr, Mn, and Ni also have relatively low formation energies, as shown in Fig. 7. This partly explains why Fe and Co hydrides are unstable at atmospheric pressure, whereas Ni hydrides are stable. Natural metal hydrides might offer a new perspective by identifying suitable geological settings on Earth.

In recent years, natural hydrogen has gained widespread attention in the energy industry as an emerging carbon-free energy source. Mali successfully explored and developed the world's first natural hydrogen well, achieving commercial success (Prinzhofer et al., 2018). Its discovery has attracted significant interest from researchers and energy companies, resulting in a sharp increase in the number of companies engaged in natural hydrogen exploration.

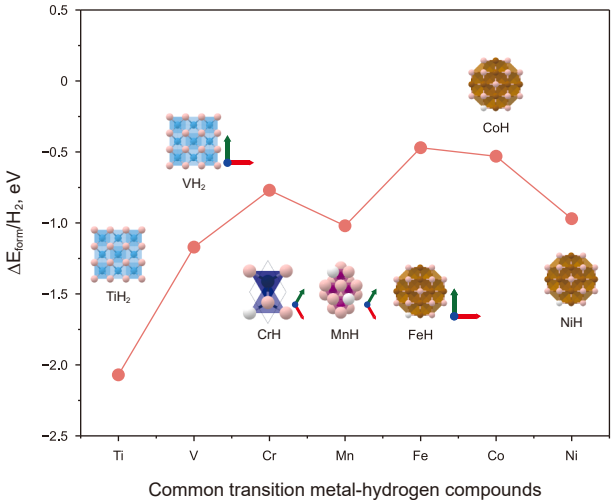

Fig. 7. Formation energies of common transition metal hydrides, modified from Smithson et al. (2002).

As of mid-2023, there were 40 active companies, compared to only 3 in 2020. However, project development has slowed in some countries due to the absence of regulatory frameworks. On the other hand, progress has been made in different countries, with Mali, the United States, France, Australia, and Spain already issuing exploration licenses (Agency, 2023). Additionally, natural metal hydrides have been discovered on the Earth's surface in Israel, where Bindi et al. (2019) reported the world's first natural metal hydride—VH_2 (Bindi et al., 2019; Warr, 2021). This could potentially lead to the exploration and exploitation of natural hydrides as an additional energy source in the future.

4. Conclusions and prospect

The discovery of vanadium hydrides as the first natural metal hydride on Earth opens new avenues for exploring and exploiting hydrides within the Earth. In this study, we experimentally investigated the high-pressure and high-temperature stability and melting behavior of the vanadium hydrides. The experimental results showed that vanadium hydrides could form at 0.8–3 GPa and 1000–1500 °C, relevant to Earth's shallow mantle, through interaction between water and vanadium metal. Therefore, we propose that metallic vanadium in the mantle reacts with subducted water at mantle temperatures and pressures to form natural vanadium hydrides, which are then transported to the surface via magmatic processes. Additionally, through molecular dynamics simulations, we determined that the melting temperature of VH_2 under 1 GPa pressure is between 1400 and 1500 °C. Indicating that the natural VH_2 may originate from Earth's shallow mantle. Our high-pressure experimental and molecular dynamics simulations also provide critical insights into understanding the formation and stability of vanadium-hydrogen compounds in Earth's mantle. They may serve as a preliminary reference for future exploration and development of natural metal hydrides for hydrogen storage.

CRediT authorship contribution statement

Yu-Tong Su: Writing – original draft, Formal analysis, Data curation. **Zhi-Jun Jin:** Writing – review & editing, Funding acquisition. **Ren-Biao Tao:** Writing – review & editing, Funding acquisition. **Jin-Tao Zhu:** Writing – review & editing, Investigation. **Run-Chao Liu:** Writing – review & editing, Methodology. **Lu Wang:** Writing – review & editing. **Hao-Zhe Zhang:** Writing – review & editing. **Shubham Choudhary:** Writing – review & editing.

Declaration of interest statement

The authors declare that they have no known competing financial interests or personal relationships that could have appeared to influence the work reported in this paper.

Acknowledgments

This research is funded by the National Natural Science Foundation of China (42488101, U25A202984, L2424218); Ordos Municipal and Provincial Government Consultation Project (KCX2024003); Frontier Interdisciplinary Research and Evaluation Project of the Chinese Academy of Sciences (5-XKC2025004).

Supplementary Information

Supplementary Information to this article can be found online at https://doi.org/10.1016/j.petsci.2026.04.006.

References

AbdKhalim Khafidz, N.Z., Yaakob, Z., Lim, K.L., Timmiati, S.N., 2016. The kinetics of lightweight solid-state hydrogen storage materials: a review. Int. J. Hydrogen Energy 41, 13131–13151. https://doi.org/10.1016/j.ijhydene.2016.05.169.
Agency, I.E., 2023. Global Hydrogen Review 2023. International Energy Agency.
Aguey-Zinsou, K.-F., Ares-Fernández, J.-R., 2010. Hydrogen in magnesium: new perspectives toward functional stores. Energy Environ. Sci. 3, 526–543. https://doi.org/10.1039/B921645F.
Bindi, L., Cámara, F., Griffin, W.L., Huang, J.-X., Gain, S.E.M., Toledo, V., O'Reilly, S.Y., 2019. Discovery of the first natural hydride. Am. Mineral. 104, 611–614. https://doi.org/10.2138/am-2019-6949.
Bindi, L., Cámara, F., Gain, S.E.M., Griffin, W.L., Huang, J.-X., Saunders, M., Toledo, V., 2020. Kishonite, VH_2, and Oreillyite, Cr_2N, two new minerals from the corundum xenocrysts of Mt Carmel, Northern Israel. Minerals 10, 1118.
Braam, M., van der Tak, F.F., Chubb, K.L., Min, M., 2021. Evidence for chromium hydride in the atmosphere of hot Jupiter WASP-31b. Astron. Astrophys. 646, A17. https://doi.org/10.1051/0004-6361/202039509.
Changeat, Q., Edwards, B., 2021. The hubble WFC3 emission spectrum of the extremely hot Jupiter KELT-9b. Astrophys. J. Lett. 907, L22. https://doi.org/10.3847/2041-8213/abd84f.
Chen, X.-Q., Wolf, W., Podloucky, R., Rogl, P., Marsman, M., 2005. Ab initio study of ground-state properties of the Laves-phase compound $TiCr_2$,$ZrCr_2$, and $HfCr_2$. Phys. Rev. B. 72, 054440. https://doi.org/10.1103/PhysRevB.72.054440.
Durbin, D., Malardier-Jugroot, C., 2013. Review of hydrogen storage techniques for on board vehicle applications. Int. J. Hydrogen Energy 38, 14595–14617. https://doi.org/10.1016/j.ijhydene.2013.07.058.
Fukai, Y., 2005. The Metal-Hydrogen System: Basic Bulk Properties. Springer-Verlag, Berlin.
Geßmann, C.K., Rubie, D.C., 1998. The effect of temperature on the partitioning of nickel, cobalt, manganese, chromium, and vanadium at 9 GPa and constraints on formation of the arth's core. Geochem. Cosmochim. Acta 62, 867–882. https://doi.org/10.1016/S0016-7037(98)00023-4.
Griffin, W.L., Gain, S.E.M., et al., 2020. Extreme reduction: Mantle-Derived oxide xenoliths from a hydrogen-rich environment. Lithos 358–359, 105404. https://doi.org/10.1016/j.lithos.2020.105404.
Grimme, S., Antony, J., Ehrlich, S., Krieg, H., 2010. A consistent and accurate ab initio parametrization of density functional dispersion correction (DFT-D) for the 94 elements H-Pu. J. Chem. Phys. 132, 154104.
Hong, Q.-J., Ushakov, S.V., van de Walle, A., Navrotsky, A., 2022. Melting Temperature Prediction Using a Graph Neural Network Model: from Ancient Minerals to New Materials, vol 119. Proceedings of the National Academy of Sciences, e2209630119.
Jain, I., Lal, C., Jain, A., 2010. Hydrogen storage in Mg: a most promising material. Int. J. Hydrogen Energy 35, 5133–5144. https://doi.org/10.1016/j.ijhydene.2009.08.088.
Jain, R., Jain, A., Agarwal, S., Lalla, N., Ganesan, V., Phase, D., Jain, I., 2007. Hydrogenation behaviour of Ce-based AB5 intermetallic compounds. J. Alloys Compd. 440, 84–88. https://doi.org/10.1016/j.jallcom.2006.08.326.
Karlsruhe, 2003. Hydrogen Energy and Fuel Cells: a Vision of our Future. European Communities.
Katsura, T., 2022. A revised adiabatic temperature profile for the mantle. J. Geophys. Res. Solid Earth 127, e2021JB023562. https://doi.org/10.1029/2021JB023562.

Kresse, G., Joubert, D., 1999. From ultrasoft pseudopotentials to the projector augmented-wave method. Phys. Rev. B 59.
Kumar, A., Muthukumar, P., Sharma, P., Kumar, E.A., 2022. Absorption based solid state hydrogen storage system: a review. Sustain. Energy Technol. Assessments 52, 102204. https://doi.org/10.1016/j.seta.2022.102204.
Kumar, S., Taxak, M., Krishnamurthy, N., Suri, A.K., Tiwari, G.P., 2012. Terminal solid solubility of hydrogen in V–Al solid solution. Int. J. Refract. Metals Hard Mater. 31, 76–81. https://doi.org/10.1016/j.ijrmhm.2011.09.009.
Kumar, S., Jain, A., Ichikawa, T., Kojima, Y., Dey, G.K., 2017. Development of vanadium based hydrogen storage material: a review. Renew. Sustain. Energy Rev. 72, 791–800. https://doi.org/10.1016/j.rser.2017.01.063.
Luo, X., Wang, J., Dooner, M., Clarke, J., 2015. Overview of current development in electrical energy storage technologies and the application potential in power system operation. Appl. Energy 137, 511–536. https://doi.org/10.1016/j.apenergy.2014.09.081.
Mao, H.K., Hu, Q., et al., 2017. When water meets iron at Earth's core–mantle boundary. Natl. Sci. Rev. 4, 870–878. https://doi.org/10.1093/nsr/nwx109.
Mazzolai, G., Coluzzi, B., et al., 2008. Hydrogen-storage capacities and H diffusion in bcc TiVCr alloys. J. Alloys Compd. 466, 133–139. https://doi.org/10.1016/j.jallcom.2007.11.040.
McDonough, W.F., 2003. 2.15 - compositional model for the Earth's core. In: Holland, H.D., Turekian, K.K. (Eds.), Treatise on Geochemistry. Pergamon, Oxford, pp. 547–568. https://doi.org/10.1016/B0-08-043751-6/02015-6.
McDonough, W.F., Sun, S.s., 1995. The composition of the Earth. Chem. Geol. 120, 223–253. https://doi.org/10.1016/0009-2541(94)00140-4.
Monkhorst, H.J., Pack, J.D., 1976. Special points for Brillouin-zone integrations. Phys. Rev. B 13, 5. https://doi.org/10.1103/PhysRevB.13.5188.
Ohtani, E., 2019. The role of water in Earth's mantle. Natl. Sci. Rev. 7, 224–232. https://doi.org/10.1093/nsr/nwz071.
Ostrooumov, M., Taran, Y., 2016. Vanadium, V – a new native element mineral from the Colima volcano, State of Colima, Mexico, and implications for fumarole gas composition. Mineral. Mag. 80, 371–382. https://doi.org/10.1180/minmag.2016.080.006.
Perdew, J.P., Burke, K., Ernzerhof, M., 1996. Generalized gradient approximation made simple. Phys. Rev. Lett. 77, 4.
Prinzhofer, A., Tahara Cissé, C.S., Diallo, A.B., 2018. Discovery of a large accumulation of natural hydrogen in Bourakebougou (Mali). Int. J. Hydrogen Energy 43, 19315–19326. https://doi.org/10.1016/j.ijhydene.2018.08.193.
Sakintuna, B., Lamari-Darkrim, F., Hirscher, M., 2007. Metal hydride materials for solid hydrogen storage: a review. Int. J. Hydrogen Energy 32, 1121–1140. https://doi.org/10.1016/j.ijhydene.2006.11.022.
Shearer, C.K., McKay, G., Papike, J.J., Karner, J.M., 2006. Valence state partitioning of vanadium between olivine-liquid: estimates of the oxygen fugacity of Y980459 and application to other olivine-phyric martian basalts. Am. Mineral. 91, 1657–1663. https://doi.org/10.2138/am.2006.2155.
Si, T.Z., Zhang, J.B., Liu, D.M., Zhang, Q.A., 2013. A new reversible Mg_3Ag–H_2 system for hydrogen storage. J. Alloys Compd. 581, 246–249. https://doi.org/10.1016/j.jallcom.2013.07.054.
Skripnyuk, V.M., Rabkin, E., 2012. Mg_3Cd: a model alloy for studying the destabilization of magnesium hydride. Int. J. Hydrogen Energy 37, 10724–10732. https://doi.org/10.1016/j.ijhydene.2012.04.065.
Smith, J.F., Peterson, D.T., 1982. The H-V (Hydrogen-Vanadium) system. Bulletin of Alloy Phase Diagrams 3, 55–60. https://doi.org/10.1007/BF02873412.
Smithson, H., Marianetti, C.A., Morgan, D., Van der Ven, A., Predith, A., Ceder, G., 2002. First-principles study of the stability and electronic structure of metal hydrides. Phys. Rev. B 66, 144107. https://doi.org/10.1103/PhysRevB.66.144107.
Sun, J., Liu, P., Wang, M., Liu, J., 2020. Molecular dynamics simulations of melting iron nanoparticles with/without defects using a Reaxff reactive Force field. Sci. Rep. 10, 3408. https://doi.org/10.1038/s41598-020-60416-5.
Suzuki, T., Akimoto, S.-i., Yagi, T., 1989. Metal-silicate-water reaction under high pressure. I. Formation of metal hydride and implications for composition of the core and mantle. Phys. Earth Planet. Inter. 56, 377–388. https://doi.org/10.1016/0031-9201(89)90171-4.
Tagawa, S., Sakamoto, N., Hirose, K., Yokoo, S., Hernlund, J., Ohishi, Y., Yurimoto, H., 2021. Experimental evidence for hydrogen incorporation into Earth's core. Nat. Commun. 12, 2588. https://doi.org/10.1038/s41467-021-22035-0.
Takahashi, E., 1986. Melting of a dry peridotite KLB-1 up to 14 GPa: implications on the Origin of peridotitic upper mantle. J. Geophys. Res. Solid Earth 91, 9367–9382. https://doi.org/10.1029/JB091iB09p09367.
Thompson, E.C., Davis, A.H., et al., 2018. High-pressure geophysical properties of Fcc phase FeHX. G-cubed 19, 305–314. https://doi.org/10.1002/2017GC007168.
Tseng, Y.-S., Retita, I., Andrews, J., Liang, D., Chan, S.L.I., 2023. Tailor-designed vanadium alloys for hydrogen storage in remote area and movable power supply systems. J. Energy Storage 68, 107659. https://doi.org/10.1016/j.est.2023.107659.
Umemoto, K., Hirose, K., 2015. Liquid iron-hydrogen alloys at outer core conditions by first-principles calculations. Geophys. Res. Lett. 42, 7513–7520. https://doi.org/10.1002/2015GL065899.
van Keken, P.E., Hacker, B.R., Syracuse, E.M., Abers, G.A., 2011. Subduction factory: 4. Depth-dependent flux of H2O from subducting slabs worldwide. J. Geophys. Res. Solid Earth 116. https://doi.org/10.1029/2010JB007922.
Wang, H., Huismans, R.S., Rondenay, S., 2019. Water migration in the subduction mantle wedge: a two-phase flow approach. J. Geophys. Res. Solid Earth 124, 9208–9225. https://doi.org/10.1029/2018JB017097.
Wang, W., Li, Y., Brodholt, J.P., Vočadlo, L., Walter, M.J., Wu, Z., 2021. Strong shear softening induced by superionic hydrogen in Earth's inner core. Earth Planet Sci. Lett. 568, 117014. https://doi.org/10.1016/j.epsl.2021.117014.
Warr, L.N., 2021. IMA–CNMNC approved mineral symbols. Mineral. Mag. 85, 291–320. https://doi.org/10.1180/mgm.2021.43.
Yuan, L., Steinle-Neumann, G., 2020. Strong sequestration of hydrogen into the Earth's core during planetary differentiation. Geophys. Res. Lett. 47 e2020GL088303. https://doi.org/10.1029/2020GL088303.
Yue, M., Lambert, H., Pahon, E., Roche, R., Jemei, S., Hissel, D., 2021. Hydrogen energy systems: a critical review of technologies, applications, trends and challenges. Renew. Sustain. Energy Rev. 146, 111180. https://doi.org/10.1016/j.rser.2021.111180.
Zhang, Y., Tan, Y., et al., 2020. Melting curve of vanadium up to 256 GPa: consistency between experiments and theory. Phys. Rev. B 102, 214104. https://doi.org/10.1103/PhysRevB.102.214104.
Zhao, X.Y., Yang, X.B., Ouyang, L., Zhao, Y.J., 2019. Theoretical study of M–H (M=Ti, V, Zr or Nb) structure phase diagram at high pressures. Int. J. Hydrogen Energy 44, 13592–13605. https://doi.org/10.1016/j.ijhydene.2019.03.210.